

1 **The strategies of water-carbon regulation of plants in a subtropical**
2 **primary forest on Karst soils in China**

3
4
5
6
7
8
9
10
11
12
13
14
15
16
17
18
19
20
21
22
23
24
25
26
27
28
29

Jing Wang^{1,2,3}; Xuefa Wen^{1,2*}, Xinyu Zhang^{1,2*}, Shenggong Li^{1,2}

1 Key Laboratory of Ecosystem Network Observation and Modeling, Institute of Geographic
Sciences and Natural Resources Research, Chinese Academy of Sciences, Beijing 100101, China

2 College of Resources and Environment, University of Chinese Academy of Sciences, Beijing
100190, China

3 School of Life Sciences, Beijing Normal University, Beijing 100875, China

*Correspondence: Xuefa Wen (Email: wenxf@igsnr.ac.cn. Phone +86-010-64889272)
and Xinyu Zhang (zhangxy@igsnr.ac.cn. Phone +86-10-64889679)

30 **Abstract:**

31 Coexisting plant species in a Karst ecosystem may use diversity strategies of trade off
32 between carbon gain and water loss to adopt to the low soil nutrient and water
33 availability conditions. Understanding of the impact of CO₂ diffusion and maximum
34 carboxylase activity of Rubisco (V_{cmax}) on the light-saturated net photosynthesis (A)
35 and intrinsic water use efficiency (iWUE) can provide insight into physiological
36 strategies of water-carbon regulation of coexisting plant species used in adaptation to
37 Karst environments at the leaf scale. We selected 63 dominant species (across 6 life
38 forms) in a subtropical Karst primary forest in southwestern China, measured their
39 CO₂ response curves, and calculated the corresponding stomatal conductance to CO₂
40 (g_s), mesophyll conductance to CO₂ (g_m), and V_{cmax} . The results showed that g_s and g_m
41 varied about 7.6- and 34.5-fold, respectively, and g_s was positively related to g_m . The
42 contribution of g_m to leaf CO₂ gradient was similar to that of g_s . g_s/A , g_m/A and g/A
43 was negative related to V_{cmax}/A . The relative limitations of g_s (l_s), g_m (l_m) and V_{cmax} (l_b)
44 to A for the whole group (combined 6 life forms) were significantly different from
45 each other ($P < 0.05$). l_m was the largest (0.38 ± 0.12), followed by l_b (0.34 ± 0.14) and
46 l_s (0.28 ± 0.07). No significant difference was found between l_s , l_m , and l_b for Trees
47 and Tree/shrubs, while l_m was the largest, followed by l_b and l_s for Shrubs, Grasses,
48 Viens and Ferns ($P < 0.05$). iWUE varied about 3-fold (from 29.52 to 88.92 $\mu\text{mol CO}_2$
49 $\text{mol}^{-1} \text{H}_2\text{O}$) across all species, and was significantly correlated with g_s , V_{cmax} , g_m/g_s ,
50 and V_{cmax}/g_s . These results indicated that Karst plants maintained relatively high A and
51 low iWUE through the co-variation of g_s , g_m , and V_{cmax} as adaptation to Karst
52 environment.

53

54 **Key words:** iWUE; mesophyll conductance; stomatal conductance; Karst critical
55 zone; V_{cmax}

56 **1 Introduction**

57 Diversity strategies of trade off between carbon gain and water loss are critical for the
58 survival of coexisting plant species. In order to adapt to the harsh environment,
59 coexisting plant species develop distinct patterns of strategies of carbon-water
60 regulation (light-saturated net photosynthesis (A) and intrinsic water use efficiency
61 (iWUE)) (Sullivan et al., 2017). iWUE is the ratio of A to stomatal conductance to
62 H_2O (g_{sw}) (Moreno-Gutierrez et al., 2012). Plants with high iWUE are better able to
63 adapt to the nutrient- and water-limited environment (Flexas et al., 2016). Due to the
64 greater hydraulic erosion and complex underground drainage network (Nie et al.,
65 2014; Chen et al., 2015), Karst soils cannot retain enough nutrients and water for
66 plant growth even though precipitation is high (1000-2000 mm) (Liu et al., 2011; Fu
67 et al., 2012; Chen et al., 2015). Understanding of the impact of CO_2 diffusion and
68 maximum carboxylase activity of Rubisco (V_{cmax}) on A and iWUE in Karst plants can
69 provide insight into physiological strategies of water-carbon regulation of plants used
70 in adaptation to Karst environments at the leaf scale. Until now, variability in A and
71 iWUE has been reported only in 13 co-occurring trees and 12 vines (Chen et al.,
72 2015), and 12 co-occurring tree species (Fu et al., 2012) in two tropical Karst forests
73 in southwestern China.

74

75 Based on Fick's first law, A has been shown to be limited only by leaf stomatal
76 conductance to CO_2 ($g_s = g_{sw}/1.6$) and V_{cmax} (Flexas et al., 2012; Buckley and Warren,
77 2014); originally, mesophyll conductance to CO_2 (g_m) was proposed to be infinite, i.e.
78 CO_2 concentration in chloroplast (C_c) was equal to the CO_2 concentration in
79 intercellular air space (C_i). However, g_m varies greatly among species (Warren and
80 Adams, 2006; Flexas et al., 2013). Recent studies have confirmed that A was
81 constrained jointly by g_s , g_m , and V_{cmax} , and their relative contribution to A was
82 species-dependent and site-specific (Carriqui et al., 2015; Tosens et al., 2016; Galmes
83 et al., 2017; Peguero-Pina et al., 2017a; Peguero-Pina et al., 2017b;
84 Veromann-Jurgenson et al., 2017).

85

86 Variation in iWUE ($=A/g_{sw}$) depends on the relative changes in A (g_s , g_m , V_{cmax}) and
87 g_{sw} ($g_{sw}=1.6g_s$) (Flexas et al., 2013; Gago et al., 2014). Theoretical relationships
88 between iWUE and g_s , g_m , and V_{cmax} have been deduced using two approaches. Based
89 on Fick's first law of CO₂ diffusion, Flexas et al. (2013) deduced that iWUE was a
90 function of g_m/g_s and CO₂ gradients (C_a-C_c) within a leaf. On the other hand,
91 combining Fick's first law of CO₂ diffusion and Farquhar biochemical model
92 (Farquhar and Sharkey, 1982), Flexas et al. (2016) deduced that iWUE was a function
93 of V_{cmax}/g_s , C_c , CO₂ compensation point of photosynthesis (Γ^*), and the effective
94 Michaelis–Menten constant of Rubisco for CO₂ (K_m). Until now, most previous
95 studies focused on the role of CO₂ diffusion in limiting iWUE, and suggested that
96 iWUE was negatively related to g_s , and positively related to g_m/g_s (Flexas et al., 2013).
97 Gago et al. (2014) used a meta-analysis with 239 species, and were the first to
98 confirm that iWUE was positively related to V_{cmax}/g_s . Although both g_m/g_s and
99 V_{cmax}/g_s were positively correlated with iWUE, there was only a weak correlation
100 between g_m/g_s and V_{cmax}/g_s , which indicates that iWUE can be improved by increasing
101 V_{cmax} or g_m (proportionally higher than g_s), not both (Gago et al., 2014).

102

103 It is noteworthy that Flexas et al. (2016) and Gago et al. (2014) found that most of the
104 previous work on constraints of g_s , g_m , and V_{cmax} on A were conducted in crops or
105 saplings, and only a few studies were in natural ecosystems. For example, g_m was the
106 main factor limiting A in two Antarctic vascular grasses (Saez et al., 2017), and in 35
107 Australian sclerophylls (Niinemets et al., 2009b) in different habitats. The A of two
108 closely-related Mediterranean *Abies* species growing in two different habitats was
109 mainly constrained by g_m in one, and by g_s in the other habitat (Peguero-Pina et al.,
110 2012). Beyond that, it still remains unknown how g_s , g_m , and V_{cmax} regulate A and
111 iWUE across species in natural ecosystems.

112

113 In this study, we selected 63 dominant plant species, including six life forms (Tree
114 (n=29), Tree/Shrub (n=11), Shrub (n=11), Grass (n=11), Vine (n=5), and Fern (n=3)),

115 from a subtropical primary forest in the Karst critical zone of southwestern China, and
116 measured **their** A and CO_2 response curves. g_m was calculated using the curve-fitting
117 method (Ethier and Livingston, 2004). The obtained g_m was used to transform the
118 $A-C_i$ into $A-C_c$ response curves, and then to calculate the A and $V_{c_{\max}}$. Our objective
119 was to determine and distinguish the limitations of CO_2 diffusion (g_s and g_m) and
120 $V_{c_{\max}}$ on A and $i\text{WUE}$ in different life forms in this Karst primary forest, **and to**
121 **understanding the patterns of strategies of carbon-water regulation of Karst plants.**

122

123 **2 Materials and Methods**

124 **2.1 Site information**

125 This study was conducted in a subtropical primary forest ($26^\circ 14' 48''\text{N}$, $105^\circ 45' 51''\text{E}$;
126 elevation, 1460 m), located in the Karst CZ of southwestern China. This region has a
127 typical subtropical monsoon climate, with a mean annual precipitation of 1255 mm,
128 and mean annual air temperature of 15.1°C (Zeng et al., 2016). The soils are
129 characterized by a high ratio of exposed rock, shallow and nonhomogeneous soil
130 cover, and complex underground drainage networks, e.g. grooves, channels and
131 depressions (Chen et al., 2010; Zhang et al., 2011; Wen et al., 2016). Soils and soil
132 water are easily leached into underground drainage networks. Soil texture **is** silt-clay
133 loam, and soil PH **is** 6.80 ± 0.16 (Chang et al., 2018). The total nitrogen and
134 phosphorus content in soil **is** 7.30 ± 0.66 and $1.18 \pm 0.35 \text{ g Kg}^{-1}$, respectively, which
135 was similar with that of non-Karst CZs (Wang et al., in review). However, the soil
136 quantities ($16.04 \sim 61.89 \text{ Kg m}^{-2}$) and nitrogen and phosphorus storage (12.04 and 1.68
137 t hm^{-2}) **is** much lower than that of non-Karst CZs, due to the thin and heterogeneous
138 soil layer (He et al., 2008; Jobbagy et al., 2000; Lu et al., 2010; Li et al., 2008). The
139 typical vegetation type is mixed evergreen and broadleaf deciduous primary forest,
140 dominated by *Itea yunnanensis* Franch, *Carpinus pubescens* Burk., and *Lithocarpus*
141 *confinis* Huang, etc. (Wang et al., 2018).

142

143 **2.2 Leaf gas-exchange measurements**

144 In July and August 2016, 63 species (Table S1) were selected for measurements of the
145 A and CO_2 response curves. The species sampled were selected according to their
146 abundance in the study site. They are the main component of this forest, including 55
147 woody species (46 deciduous and 10 evergreen species) and 5 herb species. To
148 distinguish the strategies of water-carbon regulation of plants among different life
149 forms, those species were grouped into 6 life forms, including (1) Tree (n=29), (2)
150 Tree/Shrub (n=11), (3) Shrub (n=11), (4) Grass (n=11), (5) Vine (n=5), and (6) Fern
151 (n=3). “Tree/Shrub” is a kind of low wood plant between Tree and Shrub. Fern grow
152 in understory. Vine climb up to the shrub canopy to get light.

153

154 Details of leaf sampling and measurements of the CO_2 response curve were briefly
155 described as follows. Branches exposed to the sun were excised from the upper part of
156 the crown (Trees, Tree/Shrubs, Shrubs and Vines) or aboveground portion (Grasses,
157 Ferns), and immediately re-cut under water to maintain xylem water continuity. Back
158 into the laboratory, branches and aboveground portions were kept at 25°C for 30 min.
159 Fully-expanded and mature leaves were induced for 30 minutes at a saturating light
160 density ($1500 \mu\text{mol m}^{-2} \text{s}^{-1}$). CO_2 response curves measurements were performed
161 when A and g_s was stable. Three leaves per species were collected and measured. A
162 total of 189 leaves were collected from adult individuals of 63 species.

163

164 The CO_2 response curves were measured with 11 CO_2 concentration gradients in
165 chamber following the procedural guidelines described by Long and Bernacchi (2003).
166 The photosynthetic photon flux density was $1500 \mu\text{mol m}^{-2} \text{s}^{-1}$. The leaf temperature
167 was 25 °C, controlled by the block temperature. The humidity in the leaf chamber was
168 maintained at ambient condition. Leaf area, thickness (LT) and dry mass were
169 measured after the CO_2 response measurements. Leaf mass per area (LMA) was
170 calculated by dividing the corresponding dry mass by leaf area. And leaf density (LD)
171 was calculated by dividing the corresponding LMA by LT. More details were
172 described in Wang et al. (2018).

173

174 **2.3 Response curve analyses**

175 A and the corresponding g_{sw} ($g_s = g_{sw}/1.6$), C_a , and C_i were extracted from the CO₂
176 response curve under saturating light (1500 $\mu\text{mol m}^{-2} \text{s}^{-1}$) conditions, with CO₂
177 concentration inside the cuvette set to 400 $\mu\text{mol mol}^{-1}$ (Domingues et al., 2010). V_{cmax}
178 was estimated by fitting A- C_c curves (Ethier and Livingston, 2004). The obtained
179 values of g_m were used to transform the A- C_i into A- C_c response curves as $C_c = C_i -$
180 A/g_m .

181

182 Three methods are most commonly used for g_m estimation. Those methods have been
183 reviewed by Warren (2006) and Pons et al. (2009). Briefly, g_m can be calculated by
184 the stable isotope method (Evans, 1983; Sharkey et al., 1991; Loreto et al., 1992), J
185 method (Bongi and Loreto, 1989; Dimarco et al., 1990; Harley et al., 1992; Epron et
186 al., 1995; Laisk et al., 2005), and ‘curve-fitting’ method (Ethier and Livingston, 2004;
187 Sharkey et al., 2007). All of these methods are based on gas exchange measurements
188 (Pons et al., 2009), and some common assumptions (Warren, 2006). Thus, the
189 accuracy of each method is to some extent unknown (Warren, 2006).

190

191 g_m was estimated by the ‘curve-fitting’ method in this study. Although the
192 ‘curve-fitting’ method is less precise than the stable isotope method, the
193 ‘curve-fitting’ method is much more readily available and has been used for several
194 decades (Warren, 2006; Sharkey, 2012). Accurate measurements of A and C_i is a
195 prerequisite for estimating g_m using the ‘curve-fitting’ method (Pons et al., 2009).
196 Warren (2006) pointed out that highly-accurate measurements need small leaf area
197 and low flow rates. We confirmed that the calculated C_c and the initial slope of A- C_c
198 curves were positive, suggesting that the measured g_m was reliable (Warren, 2006).

199

200 **2.4 Theory of trade-off between carbon and water at leaf scale**

201 The exchange of H₂O and CO₂ between the leaf and the atmosphere is regulated by
202 stomata (Gago et al., 2014). According to Fick’s first law of diffusion, A and g_s are

203 related as:

$$204 \quad A = g_s(C_a - C_i) \quad (1)$$

205 where A is the photosynthetic rate ($\mu\text{mol CO}_2 \text{ m}^{-2} \text{ s}^{-1}$); C_a is the ambient CO_2
206 concentration ($\mu\text{mol mol}^{-1}$); C_i is the intercellular CO_2 concentration ($\mu\text{mol mol}^{-1}$).

207

208 **Mesophyll** is the barrier for CO_2 inside the leaf. A and mesophyll conductance to CO_2
209 (g_m) are related as:

$$210 \quad A = g_m(C_i - C_c) \quad (2)$$

211 where C_c is the CO_2 concentration at the sites of carboxylation ($\mu\text{mol mol}^{-1}$). C_c not
212 only depends on CO_2 supply by g_m , but also on CO_2 demand (the maximum
213 carboxylase activity of Rubisco, V_{cmax}).

214

215 **(1) The relationship between iWUE and g_m/g_s**

216 iWUE is a function of CO_2 diffusion conductances (e.g. g_s and g_m) and leaf CO_2
217 concentration gradients. We can express A as the product of the total CO_2 diffusion
218 conductance (g_t) from ambient air to chloroplasts, and the corresponding CO_2
219 concentration gradients by combining Eq. (1) and (2) (Flexas et al., 2013):

$$220 \quad A = g_t [(C_a - C_i) + (C_i - C_c)] \quad (3)$$

221 where $g_t = 1/(1/g_s + 1/g_m)$. This equation demonstrates that CO_2 concentration gradients
222 in leaves are constrained by stomatal and mesophyll resistance to CO_2 . Therefore,
223 iWUE can be expressed as:

$$224 \quad \frac{A}{g_{\text{sw}}} = \frac{1}{1.6} \left(\frac{g_m/g_s}{1 + g_m/g_s} \right) [(C_a - C_i) + (C_i - C_c)] \quad (4)$$

226 Eq. (4) means that iWUE is positively related to g_m/g_s , but not to g_m itself (Warren
227 and Adams, 2006; Flexas et al., 2013; Buckley and Warren, 2014; Cano et al., 2014).

228

229 **(2) The relationship between iWUE and V_{cmax}/g_s**

230 When Fick's first law and the Farquhar biochemical model (Farquhar and Sharkey,
231 1982) are combined, iWUE is also a function of V_{cmax} . Based on the Farquhar
232 biochemical model (Farquhar and Sharkey, 1982), when A is limited by Rubisco, it

233 can be expressed by the following equation (Sharkey et al., 2007):

$$234 \quad A = \frac{V_{\text{cmax}}(C_c - \Gamma^*)}{(C_c + K_m)} - R_d \quad (5)$$

235

236 where Γ^* is the CO₂ compensation point of photosynthesis in the absence of
 237 non-photorespiratory respiration in light (R_d), and K_m is the effective
 238 Michaelis–Menten constant of Rubisco for CO₂. Combining Eq. (1) and (5) (Flexas et
 239 al., 2016), we obtain:

$$240 \quad \frac{V_{\text{cmax}}}{g_s} = \frac{(C_c + K_m)(C_a - C_i)(A + R_d)}{(C_c - \Gamma^*)A} \quad (6)$$

242 Because R_d is much smaller than A in actively photosynthesizing leaves, V_{cmax}/g_s can
 243 be approximated as:

$$244 \quad \frac{V_{\text{cmax}}}{g_s} \approx \frac{(C_c + K_m)(C_a - C_i)}{(C_c - \Gamma^*)} = \frac{(C_c + K_m)}{(C_c - \Gamma^*)} \frac{A}{g_s} \quad (7)$$

246 Consequently, iWUE can be expressed as:

$$247 \quad \frac{A}{g_{\text{sw}}} = \frac{1}{1.6} \frac{V_{\text{cmax}}}{g_s} \frac{(C_c - \Gamma^*)}{(C_c + K_m)} \quad (8)$$

249

250 **2.5 Statistical analysis**

251 (1) Quantitative analysis of limitations on A

252 The relative contribution of g_s (l_s), g_m (l_m) and V_{cmax} (l_b) to A can be separated by a
 253 quantitative limitation model introduced by Jones (Jones, 1985) and further developed
 254 by Grassi & Magnani (2005). The sum of l_s , l_m , and l_b is 1. l_s , l_m and l_b can be
 255 calculated as:

256

$$257 \quad l_s = \frac{g_t/g_s \cdot \partial A/\partial C_c}{g_t + \partial A/\partial C_c} \quad (9)$$

258

$$259 \quad l_m = \frac{g_t/g_m \cdot \partial A/\partial C_c}{g_t + \partial A/\partial C_c} \quad (10)$$

260

$$261 \quad l_b = \frac{g_t}{g_t + \partial A/\partial C_c} \quad (11)$$

262

263 where $\partial A / \partial C_c$ was calculated as the slope of $A-C_c$ response curves over a C_c range of
264 50–100 $\mu\text{mol mol}^{-1}$. l_s , l_m and l_b have no units. A is co-limited by the three factors
265 when $l_s \approx 0.3$, $l_m \approx 0.3$ and $l_b \approx 0.4$ (Galmes, J. et al., 2017).

266

267 (2) Data analysis

268 Data were analyzed either as a whole group (six life forms combined) or by individual
269 life forms. The bivariate linear regressions of leaf gas exchange parameters were
270 performed using the standardized major axis (SMA) regression fits, and all of the data
271 were made on \log_e -transformed data (Table S2).

272

273 To test for the differences among life forms, SMA regression fits were used to
274 compare the slope of regression lines which significant relationships had already been
275 obtained. Note that Grass, Vine and Fern were not considered due to the small sample
276 size. A similar trend was obtained, and no significant difference was found between
277 life forms although significant relationships were not obtained for some bivariate
278 linear regressions. Accordingly, six life forms were grouped together to analyze the
279 strategy of water-carbon regulation of plants in the whole text.

280

281 The difference of relative limitation of g_s , g_m and V_{cmax} to A for life forms or as a
282 whole group were performed using one-way ANOVA and
283 Duncan multiple comparison. The probability of significance was defined at $p < 0.05$.

284

285 3 Results

286 3.1 Interrelation among g_s , g_m , g_t , and V_{cmax}

287 CO_2 concentration gradients in leaf were controlled by CO_2 diffusion conductance
288 and V_{cmax} . Fig. 1 shows the relationship between CO_2 gradients (C_a-C_i , C_i-C_c and
289 C_a-C_c) in leaf and the corresponding CO_2 diffusion conductance (g_s , g_m and g_t) (Fig.
290 1a-c), and between C_a-C_c and V_{cmax} (Fig. 1d). CO_2 concentration gradients (C_a-C_i ,

291 C_i-C_c and C_a-C_c) were significantly negatively associated with the corresponding CO_2
292 diffusion conductance (g_s , g_m and g_t) ($P<0.001$). V_{cmax} was positively associated with
293 C_a-C_c ($P<0.001$).

294

295 g_s , g_m , and g_t were significantly positively related to each other ($P<0.001$) (Fig. S1).
296 The contribution of g_m to leaf CO_2 gradient was similar to that of g_s . The contribution
297 of g_s ($57.51\text{--}155.13 \mu\text{mol mol}^{-1}$) to C_a-C_c ($98.50\text{--}282.94 \mu\text{mol mol}^{-1}$) varied from
298 28% to 86%, and the contribution of g_m ($18.15\text{--}179.36 \mu\text{mol mol}^{-1}$) to C_a-C_c varied
299 from 14% to 72%. But the variation range of g_m ($0.02\text{--}0.69 \text{ mol CO}_2 \text{ m}^{-2} \text{ s}^{-1}$) was 4.5
300 times that of g_s ($0.05\text{--}0.38 \text{ mol CO}_2 \text{ m}^{-2} \text{ s}^{-1}$).

301

302 No relationship was found between the CO_2 diffusion conductance (g_s , g_m , and g_t) and
303 V_{cmax} (Fig. S2). However, after normalization of g_s , g_m , g_t , and V_{cmax} for A (normalized
304 parameters are hereafter called $G_s=g_s/A$, $G_m=g_m/A$, $G_t=g_t/A$, and $V=V_{\text{cmax}}/A$), V was
305 significantly positively correlated with G_m and G_t ($P<0.001$) (Fig. 2b and c), and was
306 slightly positively correlated with G_s ($P<0.05$) (Fig. 2a), which represented the
307 trade-off between CO_2 supply and demand.

308

309 **3.2 Contribution of g_s , g_m and V_{cmax} to A**

310 The variation in A was attributed to variation in g_s , g_m , g_t , and V_{cmax} . A was positively
311 correlated with g_s (Fig. 3a), g_m (Fig. 3b), and V_{cmax} (Fig. 3c). We used the quantitative
312 limitation model (Eqs. (9), (10) and (11)) to separate g_s (l_s), g_m (l_m), and V_{cmax} (l_b)
313 **limitations** to A . l_s , l_m , and l_b were negatively associated with g_s , g_m , and V_{cmax} ,
314 **respectively** (Fig. 4). The contributions by g_s , g_m , and V_{cmax} to limiting A were
315 different for each species (Fig. S3). l_s varied **2.6-fold (from 0.17 to 0.45)**, l_m varied
316 **10.5-fold (from 0.05 to 0.55)**, and l_b varied **6.2-fold (from 0.11 to 0.68)** across
317 species. Overall, l_m (0.38 ± 0.12) was **significantly larger than l_b (0.34 ± 0.14), and l_s**
318 **(0.28 ± 0.07) ($P<0.05$).**

319

320 To further understand how A was limited by g_s , g_m , and V_{cmax} among life forms, we
321 grouped the 63 species into 6 life forms: Tree, Tree/Shrub, Shrub, Grass, Vine, and
322 Fern. The results showed that there was no significantly difference between l_s , l_m and
323 l_b for Trees and Tree/shrubs. l_m of Shrubs and Grasses was significantly higher than
324 that of l_s and l_b ($P < 0.05$). l_m of Vines and Ferns was significantly higher than that of l_s
325 ($P < 0.05$) (Fig. 5).

326

327 3.3 Effect of g_s , g_m and V_{cmax} on iWUE

328 iWUE varied from 29.52 to 88.92 $\mu\text{mol CO}_2 \text{ mol}^{-1} \text{ H}_2\text{O}$. In theory, iWUE is regulated
329 by g_s ($g_{sw} = 1.6g_s$), g_m , and V_{cmax} . However, a simple correlation analysis showed that
330 iWUE was negatively related to g_s (Fig. 6b), and not related to A (Fig. 6a), g_m (Fig.
331 6c), and V_{cmax} (Fig. 6d).

332 |

333 A correlation analysis was used to test how g_m/g_s and V_{cmax}/g_s affected iWUE. The
334 results showed that iWUE was positively correlated with g_m/g_s (Fig. 7a) and V_{cmax}/g_s
335 (Fig. 7b). However, there was no significant relationship between g_m/g_s and V_{cmax}/g_s .
336 iWUE was regulated by co-variation between g_s , g_m and V_{cmax} .

337

338 4 Discussion

339 4.1 Co-variation in g_s , g_m and V_{cmax} in regulating A

340 A was constrained by g_s , g_m , and V_{cmax} acting together, however, variability in the
341 relative contribution of these three factors depended on species and habitats (Tosens
342 et al., 2016; Galmes et al., 2017; Peguero-Pina et al., 2017a; Veromann-Jurgenson et
343 al., 2017). A was significantly correlated with g_s , g_m , and V_{cmax} (Fig.3a-c). g_s was
344 positively related to g_m (Fig.S1c), while no relationship was found between the CO_2
345 diffusion conductance (g_s and g_m) and V_{cmax} (Fig. S2). The relative limitations of g_s ,
346 g_m , and V_{cmax} were separated by a quantitative limitation model (Jones, 1985; Grassi
347 & Magnani, 2005). The results showed that l_s , l_m and l_b of 63 species varied in a large
348 range (Fig. S3), indicating plants have a diverse strategies to co-ordinate the CO_2

349 diffusion (g_s and g_m) and V_{cmax} to maintain relative high A . The order of factors
350 limitations to A was $l_m > l_b > l_s$ ($P < 0.05$) (Fig.S3). Furthermore, we tested the
351 relationship between the relative limitations and the corresponding limitation factors.
352 The results showed that l_s , l_m , and l_b were negatively associated with g_s , g_m , and V_{cmax} ,
353 respectively (Fig. 4). And the relationship was stronger for g_m - l_m ($r^2=0.65$) than
354 V_{cmax} - l_b ($r^2=0.27$) and g_s - l_s ($r^2=0.19$).

355

356 g_s was better correlated with A , while the results showed that A was more limited by
357 g_m . That could be explained by two possible reasons. Firstly, compare to the linear
358 relationship between A and g_s , a nonlinear trend has been found between A and g_m
359 when $g_m > 0.4$ (Fig. 3a, b). Secondly, leaf structure plays an important role in
360 regulating g_m and V_{cmax} , consequently, in determining A (Veromann-Jurgenson et al.,
361 2017). Negative relationships between A/LMA and LT ($r^2=0.16$, $p=0.002$), and
362 A/LMA and LT ($r^2=0.3$, $p<0.001$) have been observed (Fig. S4c,d), while A was not
363 correlated to LT and LD (Fig. S4a,b).

364

365 The importance of g_m in constraining A was variable, and depended on leaf structural
366 traits, only LMA , LT , and LD were analyzed in this study. Large variability in g_m has
367 been shown both between and within species with different life forms and habits
368 (Gago et al., 2014; Flexas et al., 2016). Variability in g_m in this study is similar to that
369 in global datasets (Gago et al., 2014; Flexas et al., 2016). There was no significantly
370 difference among life forms ($P > 0.05$). Previous studies have confirmed that LMA
371 (Tomas et al., 2013), thickness of leaf cell wall (Peguero-Pina et al., 2017b), liquid
372 phase of mesophyll (Veromann-Jurgenson et al., 2017), cell wall thickness of
373 mesophyll (Terashima et al., 2011; Tosens et al., 2016), and surface area of mesophyll
374 and chloroplast exposed to intercellular space (Veromann-Jurgenson et al., 2017)
375 were the main limitations for g_m . The wide variability of g_m between different species
376 and life forms in the same ecosystem seems to be related to the diversity of leaf
377 anatomical traits.

378

379 No significant difference of LMA, LT, and LD was found among life forms ($P < 0.05$).
380 The negative correlation of g_m (Terashima et al., 2005) or g_m/LMA (Niinemets et al.,
381 2009; Veromann-Jurgenson et al., 2017) with LMA have been reported. In this study,
382 there was a significant relationship between g_m/LMA with LMA ($P < 0.01$), however,
383 no relationship was found between g_m with LMA. g_m/LMA was significantly negative
384 related to LD ($p < 0.01$) (Fig. S5c), and weak negative related to LT ($p = 0.06$) (Fig.
385 S5d), demonstrating that the negative role of cell wall thickness on g_m (Terashima et
386 al., 2006; Niinemets et al., 2009). The strong investment in supportive structures was
387 the main reason for the limitation of g_m on A (Veromann-Jurgenson et al., 2017).
388 However, it is still unknown how leaf anatomical traits affect g_m and A , and this
389 should be further explored.

390

391 g_s is responsible for CO_2 exchange between atmosphere and leaf, and regulate the
392 CO_2 fixation (A) and water loss (Lawson and Blatt, 2014). The variability of g_s was
393 controlled by stomatal anatomy, i.e. stomata density and size, and mesophyll demands
394 for CO_2 (Lawson and Blatt, 2014). However, the stomatal anatomy was not analyzed
395 in this study. We only focused on how the relationship between g_s and g_m regulate A .
396 Positive relationship between g_s and g_m has been observed (Flexas et al., 2013). For
397 example, the restricted CO_2 diffusion from the ambient air to chloroplast is the main
398 reason for a decreased A under water stress conditions due to both the stomatal and
399 mesophyll limitations (Olsovska et al., 2016). g_s was significantly positive related to
400 g_m for 63 species ($P < 0.001$, Fig. S1) in this study, and no difference of the slopes of
401 regression lines between g_s and g_m was found among life forms, demonstrating that A
402 was regulated by the co-variation of g_s and g_m . However, the variability of g_m and l_m
403 was larger than g_s and l_s , respectively (Fig. 1 and Fig. S3).

404

405 The wide variation range of l_b (0.11-0.68) highlighted the importance role of V_{cmax} in
406 regulating A . V_{cmax} was used to represent the CO_2 demand in photosynthetic process in
407 this study. The relative contribution of V_{cmax} to A not only depends on $C_a - C_c$, but also
408 on leaf nutrient levels. Positive relationship was found between $C_a - C_c$ and V_{cmax} (Fig.

409 1d). And the $V_{\text{cmax}}/\text{LMA}$ was co-regulated by leaf N, P and Mg content (Jing et al.
410 2018). In addition, $V_{\text{cmax}}/\text{LMA}$ was negatively related to LT ($p<0.05$) (Fig. S6c) and
411 LD ($p<0.05$) (Fig. S6d), while V_{cmax} was not correlated to LT and LD (Fig. S6a,b),
412 demonstrating that leaf structure plays an important role in regulating V_{cmax} .

413

414 The trade-off between CO_2 supply (g_s and g_m) and demand (carboxylation capacity of
415 Rubisco) can help maintain **relative high A** (Galmes et al., 2017; Saez et al., 2017). In
416 this study, we used V_{cmax} as a proxy for the carboxylation capacity of Rubisco, and the
417 normalized V_{cmax} by A ($V=V_{\text{cmax}}/A$) was significantly negatively correlated with the
418 normalized g_t by A ($G_t =g_t/A$) ($P<0.001$) (Fig. 2c), indicating that the trade-off
419 between CO_2 supply and demand also existed among different species in the same
420 ecosystems. For genus *Limonium* (flowering plants) (Galmes et al., 2017), g_t was
421 significantly positively related to Rubisco carboxylase specific activity, and
422 significantly negatively related to Rubisco specificity factor to CO_2 . In case of
423 Antarctic vascular (Saez et al., 2017) and Mediterranean plants (Flexas et al., 2014), A
424 was mainly limited by low g_m , but it could be partially counterbalanced by a **highly**
425 **efficient** Rubisco through high specificity for CO_2 . This highlights the importance of
426 the trade-off between CO_2 supply and demand in plant adaptation to Karst
427 environment. However, it is still unknown how leaf anatomical traits affect g_m , V_{cmax}
428 and A, and this should be further explored.

429

430 **4.2 Co-variation of g_s , g_m and V_{cmax} in regulating iWUE**

431 Compared with the global dataset under well-watered conditions (19.27-171.88 μmol
432 $\text{CO}_2 \text{ mol}^{-1} \text{ H}_2\text{O}$) (Flexas et al., 2016), iWUE ($52.85 \pm 13.08 \mu\text{mol CO}_2 \text{ mol}^{-1} \text{ H}_2\text{O}$)
433 was somewhat lower in this study. **iWUE varied from 29.53 to 88.91 $\mu\text{mol CO}_2 \text{ mol}^{-1}$**
434 **H_2O , and** the variability of iWUE was larger than in the Karst tropical primary forest
435 (Fu et al., 2012; Chen et al., 2015). The average iWUE of 12 **Vines** and 13 **Trees** in
436 the Karst tropical primary forest was $41.23 \pm 13.21 \mu\text{mol CO}_2 \text{ mol}^{-1} \text{ H}_2\text{O}$ (Chen et al.,
437 2015), while that of 6 evergreen and 6 deciduous **Trees** was 66.7 ± 4.9 and 49.7 ± 2.0

438 $\mu\text{mol CO}_2 \text{ mol}^{-1} \text{ H}_2\text{O}$, respectively (Fu et al., 2012). The results demonstrated that
439 Karst plants use a diverse strategies of carbon-water regulation to adopt to the harsh
440 Karst environment.

441

442 Coexisting species have a diversity strategies of carbon-water regulation, ranging
443 from ‘profligate/opportunistic’ to ‘conservative, that means their ecophysiological
444 niche are separate (Moreno-Gutierrez et al., 2012; Nie et al., 2014; Prentice et al.,
445 2014). Species with high g_s , and low iWUE were defined to have
446 ‘profligate/opportunistic’ water use strategy, and species with low g_s and high iWUE
447 were defined to exhibit ‘conservative’ water use strategy (Moreno-Gutierrez et al.,
448 2012). In consistent with previous study (Moreno-Gutierrez et al., 2012), coexisting
449 plant species growing in the Karst ecosystem had a diversity water use strategies.
450 However, Karst plants tended to lose more water to gain more carbon, i.e. Karst plants
451 used ‘profligate/opportunistic’ water use strategy to adopt to the low nutrient
452 availability and water stress conditions.

453

454 Prentice et al. (2014) studied the trade-off between carbon gain and water loss of
455 woody species in contrasting climates, and found that species in hot and wet regions
456 tend to lose more water in order to fix more carbon (high g_s/A , low $V_{\text{cmax_Ci}}/A$), and
457 vice versa. Although Karst soils cannot contain enough water for plant growth, the
458 trade-off between carbon gain and water loss (high g_s/A and low $V_{\text{cmax_Ci}}/A$) were
459 similar to the shown for plants growing in hot and wet regions (Prentice et al., 2014).

460

461 iWUE is regulated by the co-variation of g_s , g_m , and V_{cmax} . In theory, water loss is
462 regulated by g_s only, while carbon gain (A) was regulated by g_s , g_m , and V_{cmax} (Fig. 3)
463 (Lawson and and Blatt, 2014). However, iWUE in this study was negatively related to
464 g_s ($R^2=0.30$), negatively related to V_{cmax} ($R^2=0.09$), and not related to A , g_m (Fig. 6).

465

466 CO_2 diffusion and Farquhar biochemical model indicated that iWUE is affected by
467 g_m/g_s and V_{cmax}/g_s (Gago et al., 2014; Flexas et al., 2016). There was a hyperbolic

468 dependency of iWUE on g_m/g_s due to the roles of g_s and g_m in C_i and C_c , and of C_c in
469 A (Flexas et al., 2016). In meta-analyses, both Gago et al. (2014) and Flexas et al.
470 (2016) found that iWUE was significantly positively related to g_m/g_s and V_{cmax}/g_s . The
471 results of this study are consistent with the meta-analyses (Fig. 7), demonstrating that
472 plant species with relatively high g_m/g_s or V_{cmax}/g_s had relatively high iWUE. **The**
473 **relationship between iWUE and V_{cmax}/g_s ($R^2=0.50$) was stronger than the relationship**
474 **between iWUE and g_m/g_s ($R^2=0.20$), demonstrating iWUE was mainly regulated by**
475 **V_{cmax}/g_s . The reason maybe that iWUE was correlated to g_s and V_{cmax} , and g_s was**
476 **positive related to g_m .**

477

478 However, plants cannot simultaneously have high g_m/g_s and high V_{cmax}/g_s . Similarly to
479 the study of Gago et al. (2014), we found no relationship between g_m/g_s and V_{cmax}/g_s .
480 Gago et al. (2014) thought that the poor relationship between g_m/g_s and V_{cmax}/g_s
481 indicated that the iWUE may be improved by g_m/g_s or V_{cmax}/g_s separately; if both of
482 them were simultaneously improved, the enhanced effect on iWUE could be
483 anticipated. In addition, Flexas et al. (2016) showed in a simulation that the increase
484 in iWUE caused by overinvestment in photosynthetic capacity would progressively
485 lead to inefficiency in **the** trade-off between carbon gain and water use, causing an
486 imbalance between CO_2 supply and demand.

487

488 **5 Conclusions**

489 **This study provides information of limitations of A and iWUE by g_s , g_m , and V_{cmax} in**
490 **63 species across 6 life forms in the field. The results showed that plants growing in**
491 **Karst CZs used a diverse strategies of carbon-water regulation, but no difference was**
492 **found among life forms. The co-variation of CO_2 supply (g_s and g_m) and demand**
493 **(V_{cmax}) regulated A , indicating that species maintain a relatively high A through**
494 **co-varying their leaf anatomical structure and V_{cmax} . iWUE was relatively low, but**
495 **ranged widely, indicating that plants used **the** ‘profligate/opportunistic’ water use**
496 **strategy to maintain the survival, growth, and structure of the community. iWUE was**

497 regulated by g_s , V_{cmax} , g_m/g_s and V_{cmax}/g_s , indicating that species with high g_m/g_s or
498 V_{cmax}/g_s will have to be much more competitive to response to the ongoing rapid
499 warming and drought in the Karst CZs.

500

501 **Acknowledgements**

502 This study was supported by the National Natural Science Foundation of China
503 [41571130043, 31470500, and 41671257].

504

505 **Author contributions**

506 JW, XFW. and XYZ planed and designed the research. JW performed experiments
507 and analyzed data. JW prepared the manuscript with contributions from all
508 co-authors.

509

510 **Competing interests.**

511 The authors declare that they have no conflict of interest.

512

513 **6 References**

514 Bongio, G. and Loreto, F.: Gas-exchange properties of salt-stressed olive (*Olea-Europa*
515 L) leaves, *Plant Physiol.*, 90, 1408-1416, 1989.

516 Buckley, T.N. and Warren, C.R.: The role of mesophyll conductance in the economics
517 of nitrogen and water use in photosynthesis, *Photosynthesis Res.*, 119, 77-88,
518 2014.

519 Chang, J.J., Zhu, J.X., Xu, L., Su, H.X., Gao, Y., Cai, X.L., Peng, T., Wen, X.F.,
520 Zhang, J.J., He, N.P.: Rational land-use types in the karst regions of China:
521 Insights from soil organic matter composition and stability, *Catena*, 160, 345-353,
522 2018.

523 Cano, F.J., Lopez, R. and Warren, C.R.: Implications of the mesophyll conductance to
524 CO₂ for photosynthesis and water-use efficiency during long-term water stress
525 and recovery in two contrasting *Eucalyptus* species, *Plant Cell Environ.*, 37,
526 2470-2490, 2014.

527 Carriqui, M., Cabrera, H.M., Conesa, M.A., Coopman, R.E., Douthe, C., Gago, J.,
528 Galle, A., Galmes, J., Ribas-Carbo, M., Tomas, M. and Flexas, J.: Diffusional
529 limitations explain the lower photosynthetic capacity of ferns as compared with
530 angiosperms in a common garden study, *Plant Cell Environ.*, 38, 448-460, 2015.

531 Chen, H., Zhang, W., Wang, K. and Fu, W.: Soil moisture dynamics under different
532 land uses on karst hillslope in northwest Guangxi, China, *Environ. Earth Sci.*, 61,
533 1105-1111, 2010.

534 Chen, P. and Zhou, Y.: Soil nutrient capacity and forest tree sustainability in plateau
535 Karst region. *Earth and Environment*, 45, 32-37, 2017. (In Chinese)

536 Chen, Y.J., Cao, K.F., Schnitzer, S.A., Fan, Z.X., Zhang, J.L. and Bongers, F.:
537 Water-use advantage for lianas over trees in tropical seasonal forests, *New*
538 *Phytol.*, 205, 128-136, 2015.

539 Dimarco, G., Manes, F., Tricoli, D. and Vitale, E.: Fluorescence Parameters Measured
540 Concurrently with Net Photosynthesis to Investigate Chloroplastic CO₂
541 Concentration in Leaves of *Quercus ilex* L, *J. Plant Physiol.*, 136, 538-543, 1990.

542 Domingues, T.F., Meir, P., Feldpausch, T.R., Saiz, G., Veenendaal, E.M., Schrod, F.,
543 Bird, M., Djagbletey, G., Hien, F., Compaore, H., Diallo, A., Grace, J. and Lloyd,
544 J.: Co-limitation of photosynthetic capacity by nitrogen and phosphorus in West
545 Africa woodlands, *Plant Cell Environ.*, 33, 959-980, 2010.

546 Epron, D., Godard, D., Cornic, G. and Genty, B.: Limitation of net CO₂ assimilation
547 rate by internal resistances to CO₂ transfer in the leaves of two tree species
548 (*Fagus sylvatica* L. and *Castanea sativa* Mill), *Plant Cell Environ.*, 18, 43-51,
549 1995.

550 Ethier, G.J. and Livingston, N.J.: On the need to incorporate sensitivity to CO₂
551 transfer conductance into the Farquhar-von Caemmerer-Berry leaf
552 photosynthesis model, *Plant Cell Environ.*, 27, 137-153, 2004.

553 Evans, J.R.: Nitrogen and photosynthesis in the flag leaf of Wheat (*Triticum aestivum*
554 L.), *Plant Physiol.*, 72, 297-302, 1983.

555 Evans, J.R. and Voncaemmerer, S.: Carbon dioxide diffusion inside leaves, *Plant*
556 *Physiol.*, 110, 339-346, 1996.

557 Farquhar, G.D. and Sharkey, T.D.: Stomatal conductance and photosynthesis, *Annu.*
558 *Rev. Plant Physiol. Plant Mol. Biol.*, 33, 317-345, 1982.

559 Flanagan, L.B. and Farquhar, G.D.: Variation in the carbon and oxygen isotope
560 composition of plant biomass and its relationship to water-use efficiency at the
561 leaf- and ecosystem-scales in a northern Great Plains grassland, *Plant Cell*
562 *Environ.*, 37, 425-438, 2014.

563 Flexas, J., Barbour, M.M., Brendel, O., Cabrera, H.M., Carriqui, M., Diaz-Espejo, A.,
564 Douthe, C., Dreyer, E., Ferrio, J.P., Gago, J., Galle, A., Galmes, J., Kodama, N.,
565 Medrano, H., Niinemets, U., Peguero-Pina, J.J., Pou, A., Ribas-Carbo, M.,
566 Tomas, M., Tosens, T. and Warren, C.R.: Mesophyll diffusion conductance to
567 CO₂: An unappreciated central player in photosynthesis, *Plant Sci.*, 193, 70-84,
568 2012.

569 Flexas, J., Niinemets, U., Galle, A., Barbour, M.M., Centritto, M., Diaz-Espejo, A.,
570 Douthe, C., Galmes, J., Ribas-Carbo, M., Rodriguez, P., Rossello, F.,
571 Soolanayakanahally, R., Tomas, M., Wright, I.J., Farquhar, G.D. and Medrano, H.:
572 Diffusional conductances to CO₂ as a target for increasing photosynthesis and
573 photosynthetic water-use efficiency, *Photosynthesis Res.*, 117, 45-59, 2013.

574 Flexas, J., Diaz-Espejo, A., Gago, J., Galle, A., Galmes, J., Gulias, J. and Medrano, H.:
575 Photosynthetic limitations in Mediterranean plants: A review, *Environ. Exp. Bot.*,
576 103, 12-23, 2014.

577 Flexas, J., Diaz-Espejo, A., Conesa, M.A., Coopman, R.E., Douthe, C., Gago, J.,
578 Galle, A., Galmes, J., Medrano, H., Ribas-Carbo, M., Tomas, M. and Niinemets,
579 U.: Mesophyll conductance to CO₂ and Rubisco as targets for improving intrinsic
580 water use efficiency in C-3 plants, *Plant Cell Environ.*, 39, 965-982, 2016.

581 Fu, P.-L., Jiang, Y.-J., Wang, A.-Y., Brodribb, T.J., Zhang, J.-L., Zhu, S.-D. and Cao,
582 K.-F.: Stem hydraulic traits and leaf water-stress tolerance are co-ordinated with
583 the leaf phenology of angiosperm trees in an Asian tropical dry karst forest, *Ann.*
584 *Bot.*, 110, 189-199, 2012.

585 Gago, J., Douthe, C., Florez-Sarasa, I., Escalona, J.M., Galmes, J., Fernie, A.R.,
586 Flexas, J. and Medrano, H.: Opportunities for improving leaf water use

587 efficiency under climate change conditions, *Plant Sci.*, 226, 108-119, 2014.

588 Galmes, J., Angel Conesa, M., Manuel Ochogavia, J., Alejandro Perdomo, J., Francis,
589 D.M., Ribas-Carbo, M., Save, R., Flexas, J., Medrano, H. and Cifre, J.:
590 Physiological and morphological adaptations in relation to water use efficiency
591 in Mediterranean accessions of *Solanum lycopersicum*, *Plant Cell Environ.*, 34,
592 245-260, 2011.

593 Galmes, J., Molins, A., Flexas, J. and Conesa, M.A.: Coordination between leaf CO₂
594 diffusion and Rubisco properties allows maximizing photosynthetic efficiency in
595 *Limonium* species, *Plant Cell Environ.*, 40, 2081-2094, 2017.

596 Giuliani, R., Koteyeva, N., Voznesenskaya, E., Evans, M.A., Cousins, A.B. and
597 Edwards, G.E.: Coordination of leaf photosynthesis, transpiration, and structural
598 traits in rice and wild relatives (Genus *Oryza*), *Plant Physiol.*, 162, 1632-1651,
599 2013.

600 Grassi, G. and Magnani, F.: Stomatal, mesophyll conductance and biochemical
601 limitations to photosynthesis as affected by drought and leaf ontogeny in ash and
602 oak trees, *Plant Cell Environ.*, 28, 834-849, 2005.

603 Gusewell, S.: N : P ratios in terrestrial plants: variation and functional significance,
604 *New Phytol.*, 164, 243-266, 2004.

605 Harley, P.C., Loreto, F., Dimarco, G. and Sharkey, T.D.: Theoretical considerations
606 when estimating the mesophyll conductance to CO₂ flux by analysis of the
607 response of photosynthesis to CO₂, *Plant Physiol.*, 98, 1429-1436, 1992.

608 He, N.P., Yu, Q., Wu, L., Wang, Y.S. and Han, X.G.: Carbon and nitrogen store and
609 storage potential as affected by land-use in a *Leymus chinensis* grassland of
610 northern China. *Soil Biol. Biochem.* 40, 2952-2959, 2008.

611 Jobbagy, E. G. and Jackson, R. B.: The vertical distribution of soil organic carbon and
612 its relation to climate and vegetation. *Ecol. Appl.* 10, 423-436, 2000.

613 Jones, H.G.: Partitioning stomatal and non-stomatal limitations to photosynthesis,
614 *Plant Cell Environ.*, 8, 95-104, 1985.

615 Laisk, A., Eichelmann, H., Oja, V., Rasulov, B., Padu, E., Bichele, I., Pettai, H. and
616 Kull, O.: Adjustment of leaf photosynthesis to shade in a natural canopy: rate

617 parameters, *Plant Cell Environ.*, 28, 375-388, 2005.

618 Lawson, T. and Blatt, M.R.: Stomatal Size, Speed, and Responsiveness Impact on
619 Photosynthesis and Water Use Efficiency, *Plant Physiol.*, 164, 1556-1570, 2014.

620 Li, Z.P., Han, F. X., Su, Y., Zhang, T.L., Sun, B., Monts, D.L., and Plodinec, M.J.:
621 Assessment of soil organic and carbonate carbon storage in China. *Geoderma*
622 138, 119-126, 2007.

623 Liu, C.C., Liu, Y.G., Guo, K., Fan, D.Y., Yu, L.F. and Yang, R.: Exploitation of patchy
624 soil water resources by the clonal vine *Ficus tikoua* in karst habitats of
625 southwestern China, *Acta Physiol. Plant.*, 33, 93-102, 2011.

626 Long, S.P. and Bernacchi, C.J.: Gas exchange measurements, what can they tell us
627 about the underlying limitations to photosynthesis? Procedures and sources of
628 error, *J. Exp. Bot.*, 54, 2393-2401, 2003.

629 Loreto, F., Harley, P.C., Dimarco, G. and Sharkey, T.D.: Estimation of mesophyll
630 conductance to CO₂ flux by three different methods, *Plant Physiol.*, 98,
631 1437-1443, 1992.

632 Lu, X.T., Yin, J.X., Jepsen, M.R. and Tang, J.W.: Ecosystem carbon storage and
633 partitioning in a tropical seasonal forest in Southwestern China. *For. Ecol.*
634 *Manage.* 260, 1798-1803, 2010.

635 Moreno-Gutierrez, C., Dawson, T.E., Nicolas, E. and Querejeta, J.I.: Isotopes reveal
636 contrasting water use strategies among coexisting plant species in a
637 Mediterranean ecosystem, *New Phytol.*, 196, 489-496, 2012.

638 Muir, C.D., Conesa, M.A., Roldan, E.J., Molins, A. and Galmes, J.: Weak
639 coordination between leaf structure and function among closely related tomato
640 species, *New Phytol.*, 213, 1642-1653, 2017.

641 Nie, Y.P., Chen, H.S., Wang, K.L. and Ding, Y.L.: Seasonal variations in leaf $\delta^{13}\text{C}$
642 values: implications for different water-use strategies among species growing on
643 continuous dolomite outcrops in subtropical China, *Acta Physiol. Plant.*, 36,
644 2571-2579, 2014.

645 Niinemets, U., Diaz-Espejo, A., Flexas, J., Galmes, J. and Warren, C.R.: Role of
646 mesophyll diffusion conductance in constraining potential photosynthetic

647 productivity in the field, *J. Exp. Bot.*, 60, 2249-2270, 2009a.

648 Niinemets, U., Wright, I.J. and Evans, J.R.: Leaf mesophyll diffusion conductance in
649 35 Australian sclerophylls covering a broad range of foliage structural and
650 physiological variation, *J. Exp. Bot.*, 60, 2433-2449, 2009b.

651 Olsovska, K., Kovar, M., Brestic, M., Zivcak, M., Slamka, P. and Shao, H.B.:
652 Genotypically identifying Wheat mesophyll conductance regulation under
653 progressive drought stress, *Front. Plant Sci.*, DOI 10.3389/fpls.2016.01111,
654 2016.

655 Peguero-Pina, J.J., Flexas, J., Galmes, J., Niinemets, U., Sancho-Knapik, D., Barredo,
656 G., Villarroya, D. and Gil-Pelegrin, E.: Leaf anatomical properties in relation to
657 differences in mesophyll conductance to CO₂ and photosynthesis in two related
658 Mediterranean *Abies* species, *Plant Cell Environ.*, 35, 2121-2129, 2012.

659 Peguero-Pina, J.J., Siso, S., Flexas, J., Galmes, J., Garcia-Nogales, A., Niinemets, U.,
660 Sancho-Knapik, D., Saz, M.A. and Gil-Pelegrin, E.: Cell-level anatomical
661 characteristics explain high mesophyll conductance and photosynthetic capacity
662 in sclerophyllous Mediterranean oaks, *New Phytol.*, 214, 585-596, 2017a.

663 Peguero-Pina, J.J., Siso, S., Flexas, J., Galmes, J., Niinemets, U., Sancho-Knapik, D.
664 and Gil-Pelegrin, E.: Coordinated modifications in mesophyll conductance,
665 photosynthetic potentials and leaf nitrogen contribute to explain the large
666 variation in foliage net assimilation rates across *Quercus ilex* provenances, *Tree*
667 *Physiol.*, 37, 1084-1094, 2017b.

668 Perdomo, J.A., Capo-Bauca, S., Carmo-Silva, E. and Galmes, J.: Rubisco and Rubisco
669 Activase Play an Important Role in the Biochemical Limitations of
670 photosynthesis in rice, wheat, and maize under high temperature and water
671 deficit, *Front. Plant Sci.*, DOI: 10.3389/fpls.2017.00490, 2017.

672 Pons, T.L., Flexas, J., Von Caemmerer, S., Evans, J.R., Genty, B., Ribas-Carbo, M.
673 and Bruognoli, E.: Estimating mesophyll conductance to CO₂: methodology,
674 potential errors, and recommendations, *J. Exp. Bot.*, 60, 2217-2234, 2009.

675 Prentice, I.C., Dong, N., Gleason, S.M., Maire, V. and Wright, I.J.: Balancing the
676 costs of carbon gain and water transport: testing a new theoretical framework for

677 plant functional ecology, *Ecol. Lett.*, 17, 82-91, 2014.

678 Saez, P.L., Bravo, L.A., Cavieres, L.A., Vallejos, V., Sanhueza, C., Font-Carrascosa,
679 M., Gil-Pelegrin, E., Peguero-Pina, J.J. and Galmes, J.: Photosynthetic
680 limitations in two Antarctic vascular plants: importance of leaf anatomical traits
681 and Rubisco kinetic parameters, *J. Exp. Bot.*, 68, 2871-2883, 2017.

682 Sharkey, T.D., Vassey, T.L., Vanderveer, P.J. and Vierstra, R.D.: Carbon metabolism
683 enzymes and photosynthesis in transgenic tobacco (*Nicotiana tabacum* L.)
684 having excess phytochrome, *Planta*, 185, 287-296, 1991.

685 Sharkey, T.D., Bernacchi, C.J., Farquhar, G.D. and Singaas, E.L.: Fitting
686 photosynthetic carbon dioxide response curves for C3 leaves, *Plant Cell Environ.*,
687 30, 1035-1040, 2007.

688 Sharkey, T.D.: Mesophyll conductance: constraint on carbon acquisition by C3 plants,
689 *Plant Cell Environ.*, 35, 1881-1883, 2012.

690 Sun, Y., Gu, L.H., Dickinson, R.E., Pallardy, S.G., Baker, J., Cao, Y.H., Damatta, F.M.,
691 Dong, X.J., Ellsworth, D., Van Goethem, D., Jensen, A.M., Law, B.E., Loos, R.,
692 Martins, S.C.V., Norby, R.J., Warren, J., Weston, D. and Winter, K.:
693 Asymmetrical effects of mesophyll conductance on fundamental photosynthetic
694 parameters and their relationships estimated from leaf gas exchange
695 measurements, *Plant Cell Environ.*, 37, 978-994, 2014.

696 Sullivan, P. L., Wymore, A., McDowell, B., and co-authors: New Opportunities for
697 Critical Zone Science, Report of 2017 Arlington CZO All Hands Meeting
698 white booklet: Discuss new opportunities for CZ Science,
699 [http://www.czen.org/sites/default/files/CZO_2017_White_Booklet_20171015a.p](http://www.czen.org/sites/default/files/CZO_2017_White_Booklet_20171015a.pdf)
700 [df](http://www.czen.org/sites/default/files/CZO_2017_White_Booklet_20171015a.pdf), 2017.

701 Terashima, I., Araya, T., Miyazawa, S., Sone, K. and Yano, S.: Construction and
702 maintenance of the optimal photosynthetic systems of the leaf, herbaceous plant
703 and tree: an eco-developmental treatise, *Ann. Bot.*, 95, 507-519, 2005.

704 Terashima, I., Hanba, Y.T., Tazoe, Y., Vyas, P. and Yano, S.: Irradiance and phenotype:
705 comparative eco-development of sun and shade leaves in relation to
706 photosynthetic CO₂ diffusion, *J. Exp. Bot.*, 57, 343-354, 2006.

707 Terashima, I., Hanba, Y.T., Tholen, D. and Niinemets, U.: Leaf Functional Anatomy in
708 Relation to Photosynthesis, *Plant Physiol.*, 155, 108-116, 2011.

709 Tomas, M., Flexas, J., Copolovici, L., Galmes, J., Hallik, L., Medrano, H.,
710 Ribas-Carbo, M., Tosens, T., Vislap, V. and Niinemets, U.: Importance of leaf
711 anatomy in determining mesophyll diffusion conductance to CO₂ across species:
712 quantitative limitations and scaling up by models, *J. Exp. Bot.*, 64, 2269-2281,
713 2013.

714 Tosens, T., Nishida, K., Gago, J., Coopman, R.E., Cabrera, H.M., Carriqui, M.,
715 Laanisto, L., Morales, L., Nadal, M., Rojas, R., Talts, E., Tomas, M., Hanba, Y.,
716 Niinemets, U. and Flexas, J.: The photosynthetic capacity in 35 ferns and fern
717 allies: mesophyll CO₂ diffusion as a key trait, *New Phytol.*, 209, 1576-1590,
718 2016.

719 Veromann-Jurgenson, L.L., Tosens, T., Laanisto, L. and Niinemets, U.: Extremely
720 thick cell walls and low mesophyll conductance: welcome to the world of ancient
721 living!, *J. Exp. Bot.*, 68, 1639-1653, 2017.

722 Wang, J., Wen, X.F., Zhang, X.Y., Li, S.G., and Zhang, D.Y.: Magnesium enhances the
723 photosynthetic capacity of a subtropical primary forest in the Karst critical zone,
724 *SCI REP-UK*, DOI:10.1038/s41598-018-25839-1, 2018.

725 Warren, C.: Estimating the internal conductance to CO₂ movement, *Funct. Plant Biol.*,
726 33, 431-442, 2006.

727 Warren, C.R. and Adams, M.A.: Internal conductance does not scale with
728 photosynthetic capacity: implications for carbon isotope discrimination and the
729 economics of water and nitrogen use in photosynthesis, *Plant Cell Environ.*, 29,
730 192-201, 2006.

731 Wen, L., Li, D.J., Yang, L.Q., Luo, P., Chen, H., Xiao, K.C., Song, T.Q., Zhang, W.,
732 He, X.Y., Chen, H.S. and Wang, K.L.: Rapid recuperation of soil nitrogen
733 following agricultural abandonment in a karst area, southwest China,
734 *Biogeochemistry*, 129, 341-354, 2016.

735 Zeng, C., Liu, Z.H., Zhao, M. and Yang, R.: Hydrologically-driven variations in the
736 karst-related carbon sink fluxes: Insights from high-resolution monitoring of

737 three karst catchments in Southwest China, *Journal of Hydrology*, 533, 74-90,
738 2016.

739 Zhang, X.B., Bai, X.Y. and He, X.B.: Soil creeping in the weathering crust of
740 carbonate rocks and underground soil losses in the karst mountain areas of
741 southwest china, *Carbonates and Evaporites*, 26, 149-153, 2011.

742

743

744

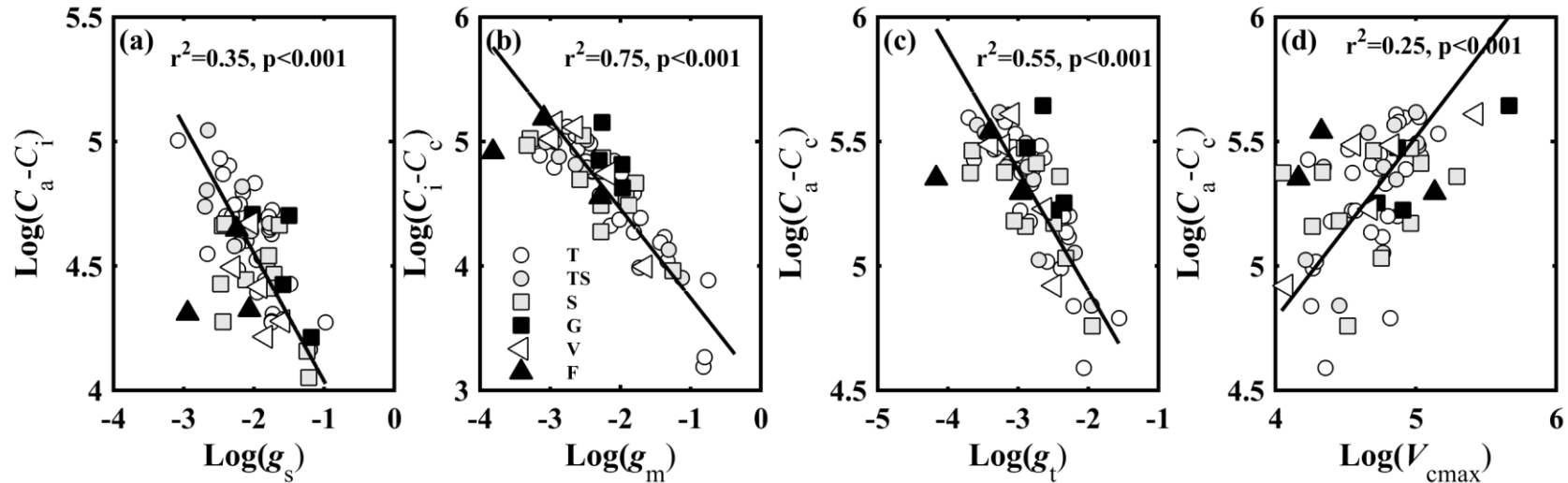
745

746

747

748 **Figures**

749

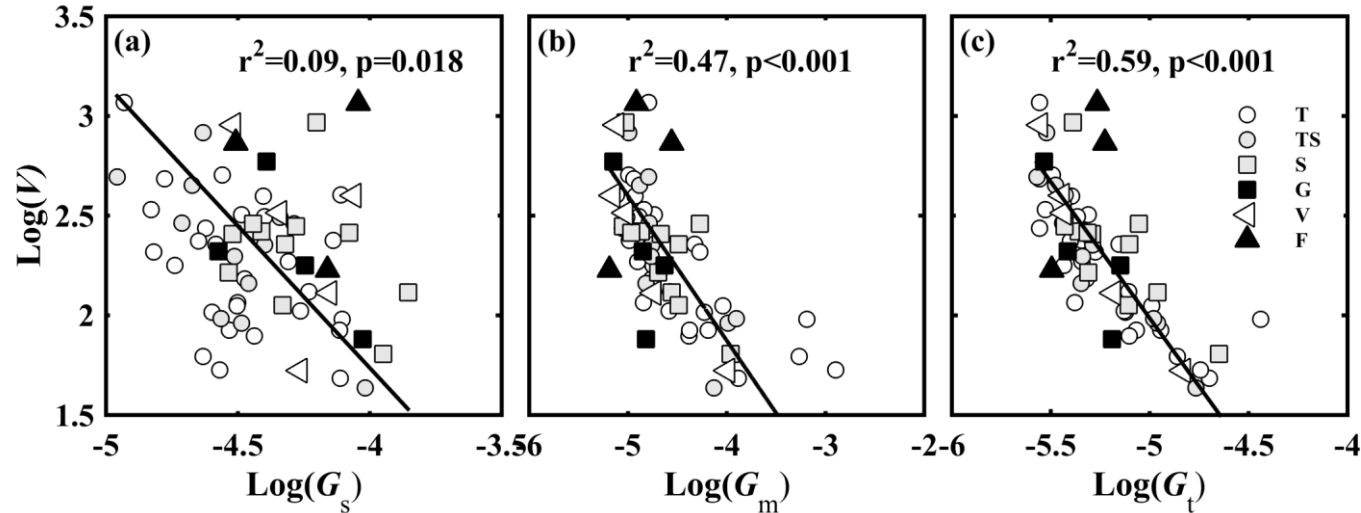


750

751 Figure 1. Relationships between (a) CO₂ gradient between ambient air and intercellular air space (C_a-C_i , $\mu\text{mol mol}^{-1}$) and stomatal conductance
 752 to CO₂ (g_s , $\text{mol CO}_2 \text{ m}^{-2} \text{ s}^{-1}$); (b) CO₂ gradient between intercellular air space and chloroplasts (C_i-C_c , $\mu\text{mol mol}^{-1}$) and mesophyll conductance to
 753 CO₂ (g_m , $\text{mol CO}_2 \text{ m}^{-2} \text{ s}^{-1}$); (c) CO₂ concentration gradient between ambient air and chloroplasts (C_a-C_c , $\mu\text{mol mol}^{-1}$) and total conductance to
 754 CO₂ (g_t , $\text{mol CO}_2 \text{ m}^{-2} \text{ s}^{-1}$); and (d) C_a-C_c and the maximum carboxylase activity of Rubisco (V_{cmax} , $\mu\text{mol CO}_2 \text{ m}^{-2} \text{ s}^{-1}$). **Lines refer to regression**
 755 **line for 63 species. T, TS, S, G, V, and F represent Tree, Tree/Shrub, Shrub, Grass, Vine, and Fern, respectively.**

756

757



758

759 Figure 2. Relationships between (a) V and G_s ; (b) V and G_m ; and (c) V and G_t . V is the ratio of photosynthetic capacity (V_{cmax}) to light-saturated
760 net photosynthesis (A , $\mu\text{mol CO}_2 \text{ m}^{-2} \text{ s}^{-1}$); G_s is the ratio of stomatal conductance to CO_2 (g_s , $\text{mol CO}_2 \text{ m}^{-2} \text{ s}^{-1}$) to A ; G_m is the ratio of mesophyll
761 conductance to CO_2 (g_m , $\text{mol CO}_2 \text{ m}^{-2} \text{ s}^{-1}$) to A ; G_t is the ratio of total conductance to CO_2 (g_t , $\text{mol CO}_2 \text{ m}^{-2} \text{ s}^{-1}$) to A . **Lines refer to regression**
762 **line for 63 species. T, TS, S, G, V, and F represent Tree, Tree/Shrub, Shrub, Grass, Vine, and Fern, respectively.**

763

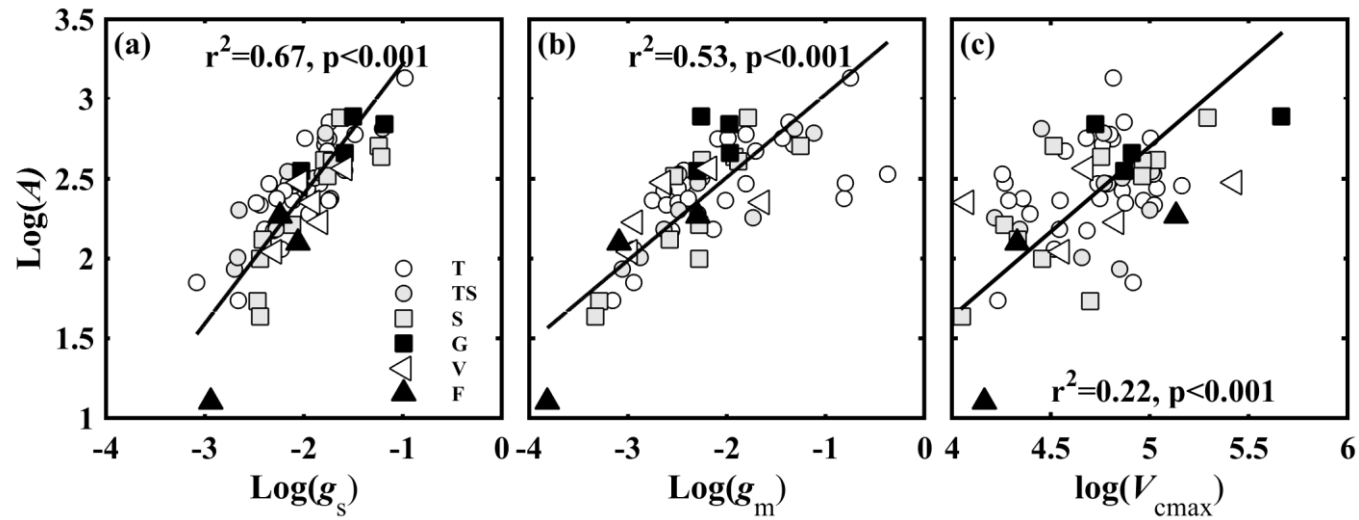
764

765

766

767

768



769

770 Figure 3. Relationships between light-saturated net photosynthesis (A , $\mu\text{mol CO}_2 \text{ m}^{-2} \text{ s}^{-1}$) and (a) stomatal conductance to CO_2 (g_s , $\text{mol CO}_2 \text{ m}^{-2}$
771 s^{-1}); (b) mesophyll conductance to CO_2 (g_m , $\text{mol CO}_2 \text{ m}^{-2} \text{ s}^{-1}$); and (c) the maximum carboxylase activity of Rubisco (V_{cmax} , $\mu\text{mol CO}_2 \text{ m}^{-2} \text{ s}^{-1}$).

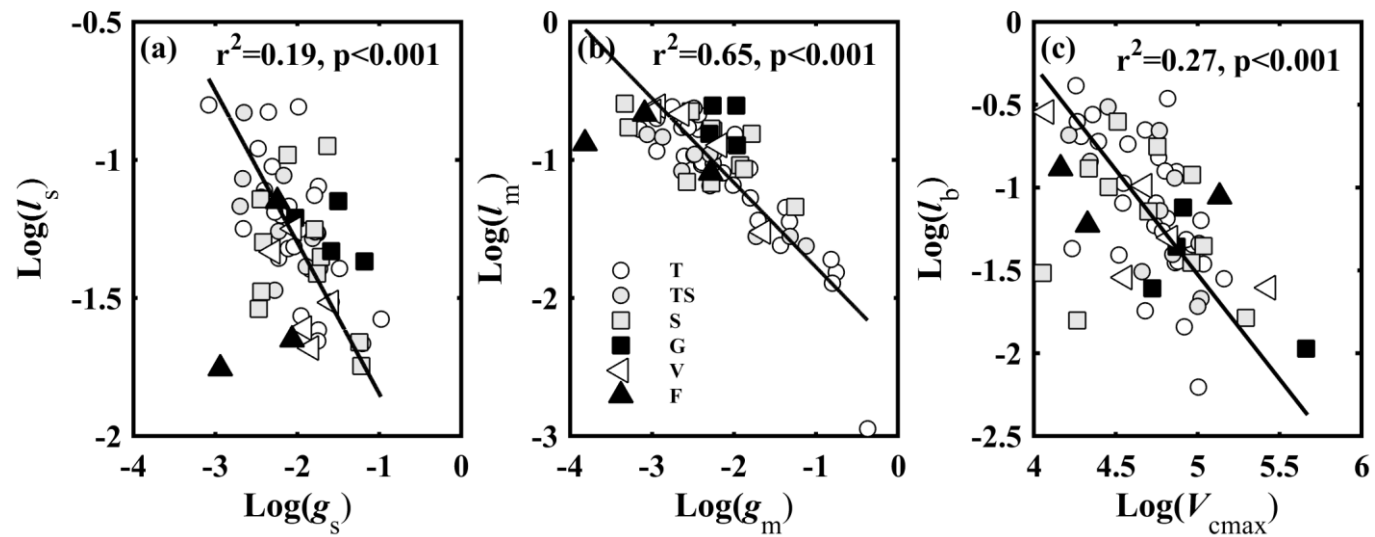
772 Lines refer to regression line for 63 species. T, TS, S, G, V, and F represent Tree, Tree/Shrub, Shrub, Grass, Vine, and Fern, respectively.

773

774

775

776



777

778 Figure 4. Relationships between (a) stomatal conductance to CO₂ (g_s , mol CO₂ m⁻² s⁻¹) and l_s (g_s limitation on light-saturated net photosynthesis
 779 (A)); (b) mesophyll conductance to CO₂ (g_m , mol CO₂ m⁻² s⁻¹) and l_m (g_m limitation on A); and (c) the maximum carboxylase activity of Rubisco
 780 (V_{cmax} , μmol CO₂ m⁻² s⁻¹) and l_b (V_{cmax} limitation on A). Lines refer to regression line for 63 species. T, TS, S, G, V, and F represent Tree,
 781 Tree/Shrub, Shrub, Grass, Vine, and Fern, respectively.

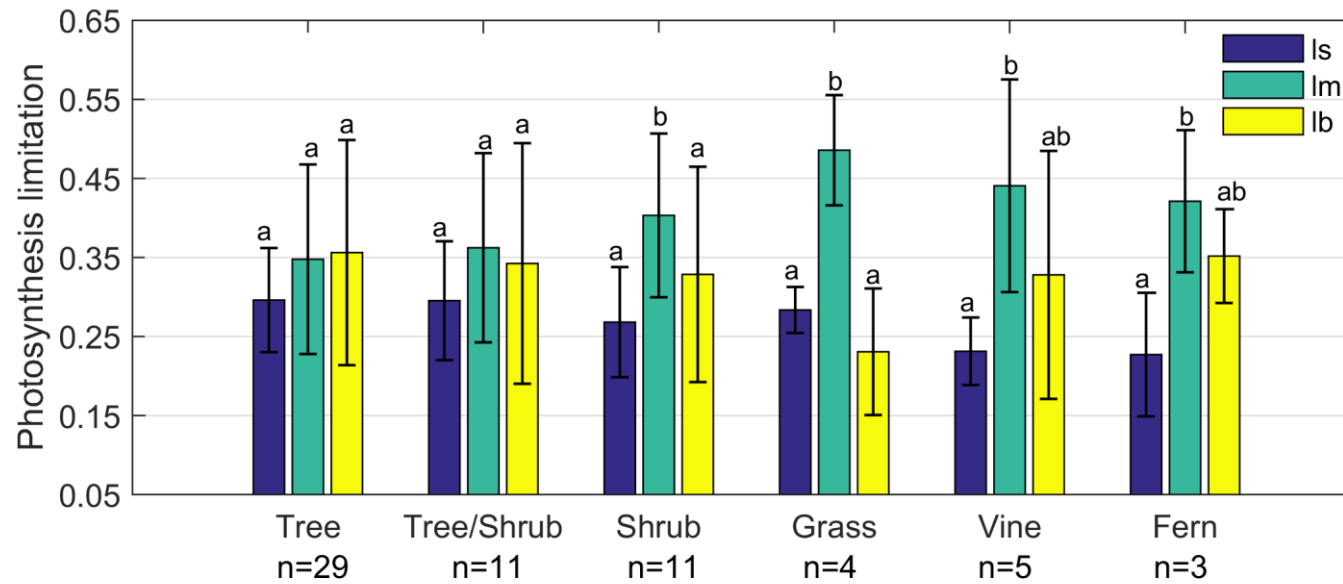
782

783

784

785

786



787

788 Figure 5. Limitation to light-saturated net photosynthesis (A) in six life forms by stomatal conductance to CO₂ (l_s), mesophyll conductance to
 789 CO₂ (l_m), and the maximum carboxylase activity of Rubisco (l_b). Error bars denominate standard deviation (1σ).

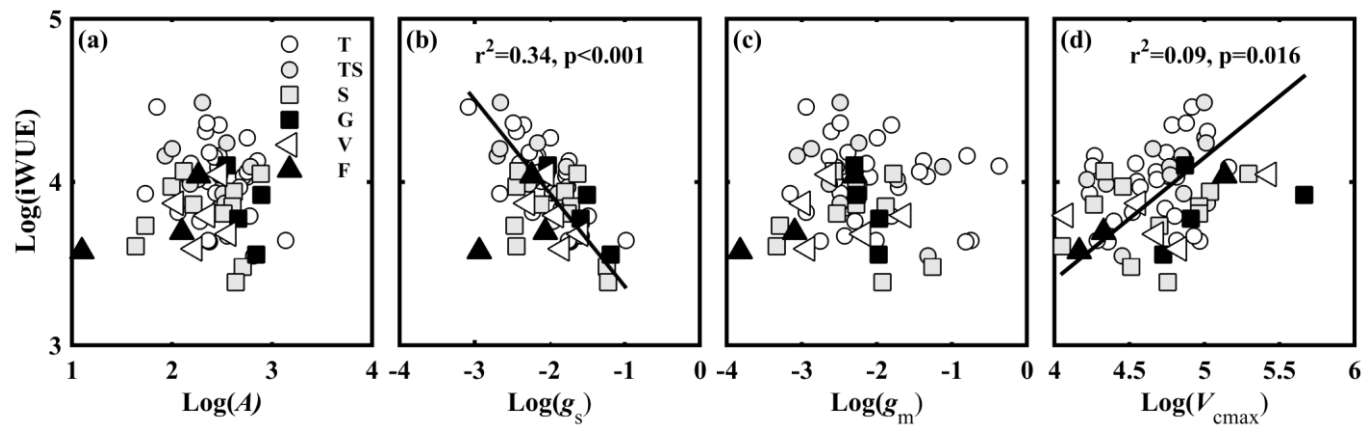
790

791

792

793

794



795

796 Figure 6. Relationships between the observed intrinsic water use efficiency ($i\text{WUE}$, $\mu\text{mol CO}_2 \text{ mol}^{-1} \text{ H}_2\text{O}$) and (a) light-saturated net
 797 photosynthesis (A , $\mu\text{mol CO}_2 \text{ m}^{-2} \text{ s}^{-1}$); (b) stomatal conductance to CO_2 (g_s , $\text{mol CO}_2 \text{ m}^{-2} \text{ s}^{-1}$); (c) mesophyll conductance to CO_2 (g_m , mol CO_2
 798 $\text{m}^{-2} \text{ s}^{-1}$) and (d) the maximum carboxylase activity of Rubisco (V_{cmax} , $\mu\text{mol CO}_2 \text{ m}^{-2} \text{ s}^{-1}$). Lines refer to regression line for 63 species. T, TS, S, G,
 799 V, and F represent Tree, Tree/Shrub, Shrub, Grass, Vine, and Fern, respectively.

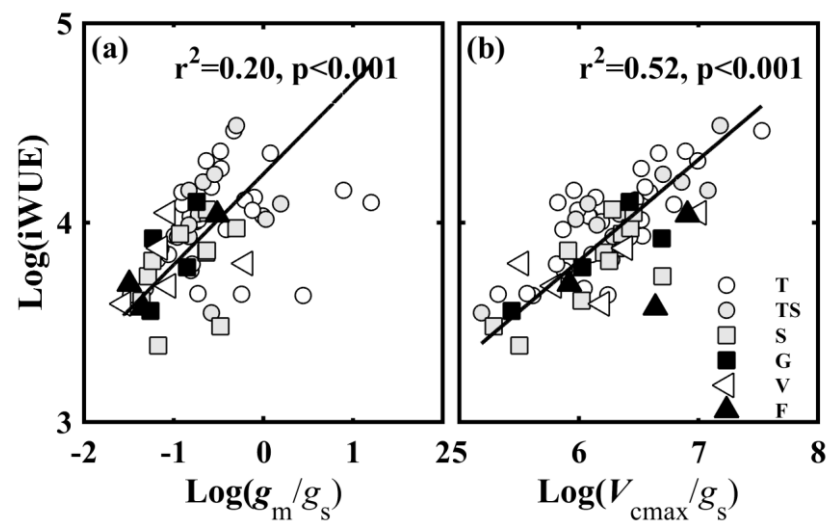
800

801

802

803

804



805

806 Figure 7. The relationships of the intrinsic water use efficiency (iWUE, $\mu\text{mol CO}_2 \text{ mol}^{-1} \text{ H}_2\text{O}$) and (a) the ratio of mesophyll conductance to CO_2

807 (g_m) to (g_s) (g_m/g_s) and (b) the ratio of the maximum carboxylase activity of Rubisco (V_{cmax}) to g_s (V_{cmax}/g_s). Lines refer to regression line for 63

808 species. T, TS, S, G, V, and F represent Tree, Tree/Shrub, Shrub, Grass, Vine, and Fern, respectively.

809